phys. stat. sol. (b) 93, 63 (1979)

Subject classification: 13.5.4; 18.2

Institut für Angewandte Festkörperphysik der Fraunhofer-Gesellschaft, Freiburg i. Br.[1])

Spin-Wave Instability Theory in Cubic Single Crystal Magnetic Insulators[2])

II. Applications[3])

By

C. E. PATTON[4])

The theory developed in Part I is used to calculate butterfly curves for parallel pumping in [001] and [110] magnetized yttrium-iron garnet and transverse pumping in [001] magnetized YIG for comparison with available experimental data. The results are in good agreement with available experimental data and resolve several previously unexplained anomalies.

Die in Teil I entwickelte Theorie wird zur Berechnung der Schmetterlingskurven für den Fall des parallelen Pumpens des in [001]- und [110]-Richtung magnetisierten Yttrium-Eisen-Granats und des senkrechten Pumpens des in [001]-Richtung magnetisierten YIG für einen Vergleich mit verfügbaren experimentellen Werten benutzt. Die Ergebnisse befinden sich in guter Übereinstimmung mit diesen experimentellen Werten und lösen einige bisher ungeklärte Anomalien.

1. Introduction

A general first-order instability theory for cubic single crystal magnetic insulators was developed in Part I of this series. The analysis was for instability processes under a generalized polarization of the microwave pump field, with the static field in any direction within the (110) plane. The purpose of Part II is to utilize this formalism to obtain theoretical results for comparison with experimental data.

Parallel pumping is considered in Section 2. It is shown that the butterfly curve for [001] magnetized yttrium-iron garnet can be accurately reproduced by including the wave vector $\boldsymbol{k}$-dependence of the spin-wave linewidth, ΔH_k, in the theoretical analysis. It is also shown that the complications which arise in the dispersion for other saturation directions combine with the k-dependence of ΔH_k to produce the curious kinks in the butterfly curves observed experimentally [1 to 3].

Subsidiary absorption or transverse pumping is considered in Section 3. Here, it also appears that the k-dependence of ΔH_k has a large effect on the shape of the theoretical butterfly curve. Specific comparisons with the data of Yakovlev et al. [4] reveal that the observed flat region over a 300 Oe interval at the bottom of the butterfly curve is due to a premature transition to $k = 0$ spin-waves. This is a direct result of the k-dependence of ΔH_k.

In the equations and discussion, all notation is identical to that used in Part I.

---

[1]) D-7800 Freiburg i. Br., BRD.

[2]) Supported in part by the U.S.A. Research Office.

[3]) Part I see phys. stat. sol. (b) 92, 211 (1979).

[4]) On sabbatical leave from Colorado State University, Fort Collins, Colorado 80523, USA, as a Research Fellow of the Alexander von Humboldt Foundation.

2. Parallel Pumping in Single Crystals

In the case of parallel pumping, we have an external microwave field described by

$$a_x = a_y = 0 , \tag{1}$$

$$a_z = 1 , \tag{2}$$

so that $\alpha_0 = 0$ is satisfied and all terms in $G_k^{(1)}$ in Part I except the $B_k^a h_0 a_z$ term vanish. The threshold field for a given (k, θ_k, φ_k) mode at $\omega_k = \omega/2$ is given by

$$h_c = \frac{\omega}{\omega_m} \frac{\Delta H_k}{\sin^2 \theta_k} \left(1 + \frac{\omega_-^2}{\omega_m^2 \sin^4 \theta_k} - \frac{2\omega_- \cos 2\varphi_k}{\omega_m \sin^2 \theta_k} \right)^{-1/2} \tag{3}$$

with $\omega_- = \gamma M A_-$. Recall that MA_- is given in (47) and Fig. 2 of Part I.

As a first application of the theory, consider the data of Yakovlev et al. [4] for parallel pumping in YIG at 9.3 GHz with the static external field in the [001] direction. Those data are shown by the solid points in Fig. 1. Recall that for the [001] direction, $\theta = 0°$ is satisfied and $\omega_- = \gamma M A_- = 0$. In this limit, the instability expression is identical to that for isotropic materials,

$$h_c = \frac{\omega}{\omega_m} \frac{\Delta H_k}{\sin^2 \theta_k} . \tag{4}$$

The dispersion constraint for $\omega_k = \omega/2$ is given by

$$\left(\frac{\omega}{2\gamma} \right) = (H_0 - 4\pi M N_z - 2H_k + Dk^2 + 4\pi M \sin^2 \theta_k) \times$$

$$\times (H_0 - 4\pi M N_z - 2H_k + Dk^2) . \tag{5}$$

A three-point fit to the data, using a trial function,

$$\Delta H_k = A + B \sin^2 (2\theta_k) + Ck , \tag{6}$$

yielded the curve indicated by the crosses in Fig. 1. The parameter A was determined to be 0.132 Oe from $h_{crit} = 0.250$ Oe at the butterfly curve minimum with $\theta_k = 90°$ and $k = 0$. The parameter B was determined to be 0.163 Oe from $h_{crit} = 0.965$ Oe at $H_0 = 1900$ Oe, for which $k = 0$ and $\theta_k = 49.4°$. The parameter C was determined to be 4.898×10^{-7} Oe cm from $h_{crit} = 0.570$ Oe at $H_0 = 1050$ Oe, for which $k = 3.52 \times 10^5$ cm^{-1} and $\theta_k = \pi/2$. These evaluations and the theoretical curve were obtained with

$$N_z = \tfrac{1}{3} \text{ (sphere)} , \qquad 4\pi M = 1750 \text{ G} , \qquad H_k = 43 \text{ Oe} ,$$

$$\gamma = 1.76 \times 10^7 \text{ Oe}^{-1} \text{ s}^{-1} , \qquad D = 5.4 \times 10^{-9} \text{ Oe cm}^2 .$$

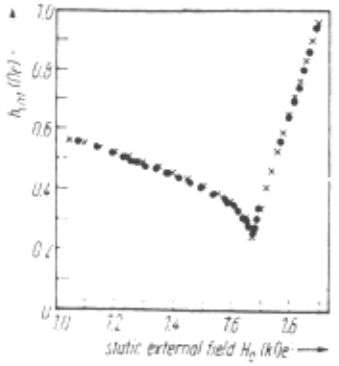

Fig. 1. Comparison of parallel pump data of Yakovlev et al. [4] for [001] magnetized YIG at 9.3 GHz with theory. ● experiment, × theory

It is seen that the fit between theory and data is almost perfect. It is to be noted that the $\sin^2(2\theta_k)$ dependence for ΔH_k provided a far superior fit to the high-field data ($H_0 > H_c$) than other simple trigonometric functions of θ_k. A contribution to ΔH_k which is linear in k is theoretically expected due to the three-magnon contribution to the spin-wave relaxation, as reviewed by Sparks [5].

As a second application of the theory, consider the configuration where anisotropy has the largest effect on both the spin-wave threshold equation and the dispersion, that is, for parallel pumping along the [110] direction. Under these conditions, the parallel pump threshold is given by

$$h_c = \frac{\omega}{\omega_m} \frac{\Delta H_k}{\sin^2 \theta_k} \times$$

$$\times \left[1 + \left(\frac{3H_k}{4\pi M \sin^2 \theta_k}\right)^2 - \left(\frac{6H_k}{4\pi M \sin^2 \theta_k}\right) \cos(2\varphi_k)\right]^{-1/2}. \tag{7}$$

The (ω/ω_m) $(\Delta H_k/\sin^2 \theta_k)$ factor is the same as for isotropic materials discussed above. The square bracket term (SBT) represents the effect of anisotropy on the parallel pump coupling for a [110] magnetized sample. The observed threshold h_{crit} will correspond to the minimum h_c when all available states at $\omega_k = \omega/2$ are considered. The SBT in (7) favours the instability of spin waves with $\varphi_k = 90°$.

The availability of spin-wave modes at $\omega_k = \omega/2$, however, is limited by the dispersion relation of (46), Part I. For a [110] magnetized sample, $MA_{xx} = H_k$, $MA_{yy} = -2H_k$, and $MA_{-} = 3H_k$ are satisfied. The schematic dispersion in Fig. 3 of Part I applies. The dispersion is shown once more in Fig. 2 for a sufficiently small applied field H_0 so that all the available states at $\omega_k = \omega/2$ have nonzero k values. As noted previously, the φ_k dependence changes the $\theta_k = 90°$ branch line of the manifold into a branch surface. The $\omega_k = \omega/2$ cut through that surface is indicated in Fig. 2. Spin waves with $\theta_k = 90°$ and $\omega_k = \omega/2$ are constrained so that k is an increasing function of φ_k. Thus, spin waves with $\varphi_k = 90°$, which from the SBT of (7) would have the lowest threshold, must also have the largest k.

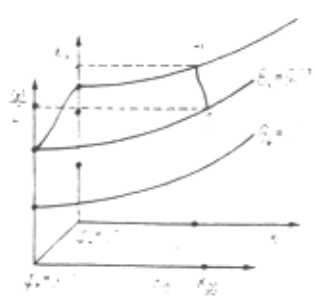

Fig. 2

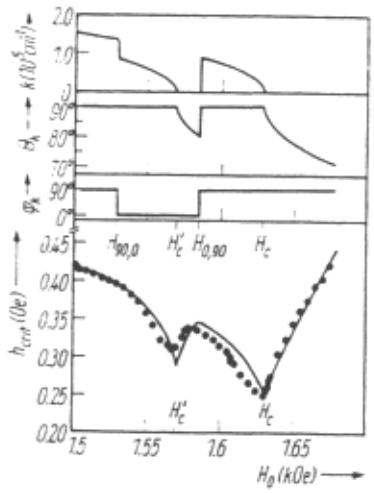

Fig. 3

Fig. 2. Schematic representation of the available spin-wave states at $\omega_k = \omega/z$ for a [110] magnetized YIG sample at low field

Fig. 3. Comparison of the parallel pump data of Sethares et al. [2] for [110] magnetized YIG at 9.522 GHz with theory. ● experimental data, ——— theory

This realization is of particular importance when the effect of the k-dependence of ΔH_k on h_{crit} is considered. Recall that ΔH_k appears in the numerator of the h_c expression of (7), and that ΔH_k increases linearly with k as indicated by (6). These considerations will tend to favour spin waves with the lowest available k value. Because of the manifold constraint in Fig. 2, this mode will have $\varphi_k = 0°$. We therefore have two opposing tendencies. The coupling favours $\varphi_k = 90°$ spin waves, while the spin-wave linewidth–k dependence combines with the dispersion constraint to favour $\varphi_k = 0°$ spin waves. At very low fields, the fractional reduction in ΔH_k at $\varphi_k = 0°$ is likely to be insufficient to have any effect, and φ_k will stick at 90°. At sufficiently high field, but still below the value where $\omega_k = \omega/2$ intersects the ($\theta_k = \pi/2$, $\varphi_k = 0°$) branch of the manifold at $k = 0$, one might expect the ΔH_k tendency to override that of the coupling and flip φ_k from 90° to zero

The data of Sethares et al. [2] for parallel pumping along [110] in a single-crystal YIG sphere support this expectation. The data obtained at a pump frequency of 9.522 GHz are shown by the solid points in Fig. 3, where the instability threshold is plotted versus the static external field. One observes the expected butterfly curve minimum at $H_0 = H_c = 1630$ Oe, which corresponds to spin waves at $\varphi_k = 90°$ in the $k = 0$ limit. In addition, one observes a secondary minimum at $H_0 = H_c' = 1570$ Oe. As pointed out in [2], but not resolved theoretically, this field would correspond to spin waves at $\varphi_k = 0°$ in the $k = 0$ limit. The data suggest, therefore, that the extra dip in the normal butterfly curve from approximately 1540 to 1580 Oe corresponds to the "flipped" φ_k of 0°.

A calculation based on a trial function,

$$\Delta H_k = A + B \sin^2(2\theta_k) + Ck + E \sin^2(2\varphi_k), \tag{8}$$

was carried out to see if a quantitative fit to the data of [2] could be obtained, and to determine the theoretical field range over which the $\varphi_k = 0°$ instability should be observable. The parameters A, B, and C were determined to be 1.137 Oe, 0.213 Oe, and 6.128 × 10⁻ Oe cm, respectively, by fitting the data to the theory for $\varphi_k = 90°$ modes at the low- and high-field limits of the data and at $H_0 = H_c$. As in the previous example, the $(A + Ck)$ term is related to three-magnon and Kasuya-LeCraw relaxation processes [5], and the $\sin^2 2\theta_k$ dependence was found to provide the best fit to the data above $H_0 = H_c$. The $\sin^2 \varphi_k$ term accounts for the empirical preference of φ_k for 0° or 90° in the field interval $H_c' < H_0 < H_c$. The parameter E was set at an arbitrary large value of 5 Oe simply to provide such a constraint on φ_k. This last term will be considered in more detail shortly.

The solid curve in Fig. 3 shows the theoretical butterfly curve that came out of the analysis. The material parameters used in the calculation were the same as noted previously. The curve is in reasonable agreement with the data. The secondary minimum is clearly in evidence. The additional curves at the top of Fig. 3 show the k, θ_k and φ_k dependences on static field for the minimum threshold mode to which h_{cr} applies. For $H_0 < H_{90°,0°}$, the reduction in ΔH_k due to the decrease in k at $\varphi_k = 0$ not sufficient to overcome the coupling preference for $\varphi_k = 90°$. As H_0 exceed $H_{90°,0°}$, however, the ΔH_k effect takes over and flips the unstable mode to $\varphi_k = 0$ This is intuitively reasonable, since the reduction in k, which is needed to maintain $\omega_k \varepsilon$ $\omega/2$ as φ_k changes from 90° to 0°, varies approximately as k^{-1}. Thus, the relative effe of the flip on ΔH_k will increase as k decreases, or as H_0 increases. As H_0 exceeds H_c', t $\varphi_k = 0°$ preference, together with the dispersion constraint, forces θ_k to decrease that h_{crit} increases. At the point $H_0 = H_{0°,90°}$, this continuing increase makes it mo favourable for φ_k and θ_k to both flip back to 90°, with the corresponding increase in

It is seen that the secondary minimum is really just the observable portion of second butterfly curve for $\varphi_k = 0°$, just as the larger field interval corresponds to t

$\varphi_k = 90°$ butterfly curve. It is to be emphasized that none of the fitted parameters in ΔH_k pertain to the secondary dip. Yet, the break points which come out of the analysis are in very good agreement with the data. As discussed in [1], this double-minimum effect is also observed for in-plane magnetized YIG slabs, saturated along [110].

The analysis does not explain why φ_k prefers only 0° or 90° in the field range between H_c' and H_c. Without the $E \sin^2(2\varphi_k)$ term in (8), the theoretical h_{crit} would simply decrease monotically from the value at H_c' to the value at H_c, with a corresponding gradual change in φ_k from 0° to 90°. The observation that φ_k sticks at 0° for $H_c' < H_0 < H_{0°,90°}$, and then flips abruptly back to 90° for $H_0 > H_{0°,90°}$ may be related to the φ_k dependence of h_c in (7). From the cos $(2\varphi_k)$ term in (7), it is seen that $\partial h_c/\partial \varphi_k$ can be zero only for $\varphi_k = 0°$ or $\varphi_k = 90°$. This means that for intermediate φ_k values, there are always nearby states with slightly different φ_k which have higher thresholds. Such nearby states may be coupled to the pumped modes by two-magnon interactions and serve as energy sinks. As a result, the observed parallel pump threshold would be for $\varphi_k = 0°$ or $\varphi_k = 90°$ modes only. Such a process may be the theoretical justification for the $E \sin^2 \varphi_k$ term in (8).

3. Transverse Pumping in Single Crystals

Theoretical butterfly curves have also been calculated for transverse pumping in single crystals for comparison with the data of Yakovlev et al. In this case, it is necessary to obtain analytical expressions for the complex uniform mode amplitudes a_{LO} and a_{AO}, or equivalently q_{LO} and q_{AO}. The expressions for q_{LO} and q_{AO} are identical to those given for q_L and q_A in [6], with the quantities X and Y suitably redefined,

$$q_{LO} = \frac{(\omega + Y)\, a_x\, e^{i\delta_x} + i(\omega + X)\, a_y\, e^{i\delta_y}}{XY - \omega^2}, \tag{9}$$

$$q_{AO} = -\frac{(\omega - Y)\, a_x\, e^{-i\delta_x} + i(\omega - X)\, a_y\, e^{-i\delta_y}}{XY - \omega^2} \tag{10}$$

with

$$X = \gamma H_x^{eff}, \tag{11}$$

$$Y = \gamma H_y^{eff}. \tag{12}$$

Expressions for H_x^{eff} and H_y^{eff} were given in Part I. For transverse pumping, the algebraic expressions are too cumbersome to obtain simple expressions for h_c as for parallel pumping. The threshold h_c for any given (k, θ_k, φ_k) combinations is obtained from equations (60), (64), and (65) of Part I.

As one application of the theory, the minimum h_c as a function of H_0 was evaluated numerically for a YIG sphere at 9.3 GHz, with H_0 parallel to [001], for comparison with the data of Yakovlev et al. [4]. The calculation was done for a linear polarized pumping field with $a_x = 1$ and $a_y = a_z = 0$. At any given field, the allowed values of θ_k and φ_k were scanned in one-degree steps in order to determine the mode with the lowest threshold. The material parameters were the same as for the parallel pump theory in Fig. 1. The results for transverse pumping are shown in Fig. 4. There are several aspects of the qualitative agreement that deserve comment. The data show a shoulder at about 1700 Oe, and a field region from 1800 to 2200 Oe where the butterfly curve is rather flat. This same effect is nicely evident in the theoretical curve as well. When one examines the behaviour of θ_k and k which comes out of the theory, the reasons for the effect are clear. It is seen that the minimum threshold in the region for $H_0 > 1700$ Oe occurs for $k = 0$ spin waves and that the θ_k actually peaks out at about 75° at $H_0 = 1700$ Oe. Thus, we have the surprising result that $k = 0$ modes are preferred over a considerable field range which extends well below the butterfly curve minimum field point at H_c.

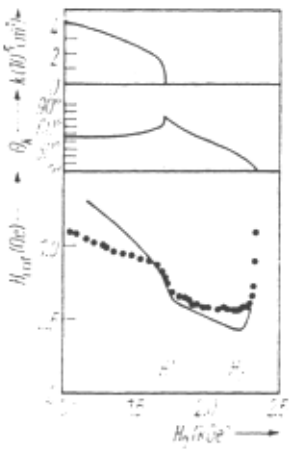

Fig. 4. Comparison of the transverse pumping data of Yakovlev et al. [4] for [001] magnetized YIG

As in the previous parallel pumping example, this result is also related to the effect of the ΔH_k k-dependence on h_{crit}. Again, there are two opposing tendencies. From the $G_k^{(1)}$ expression in Part I, the sin θ_k cos θ_k term leads to a preference of θ_k values close to 45°. Such a value would maximize $|W|$ and yield the minimum h_c value, as long as the ΔH_k k-dependence is ignored. The ΔH_k dependence on k in (6), leads, however, to a preference of low k and high θ_k. At low field and high k, the fractional reduction in ΔH_k accomplished by increasing θ_k from 45° is small, so that θ_k for the minimum threshold spin wave remains at about this value. From the insert in Fig. 4, it is seen that $\theta_k \approx 45°$ is satisfied for $H_0 \approx 1300$ Oe.

As the field is increased and the fractional decrease in ΔH_k over the allowed range of k values becomes larger, these effects cause θ_k to increase. The quantitative theoretical analysis in Fig. 4 shows that θ_k continues to increase to a value of about 75° at $H_0 = H_c' = 1700$ Oe. At this θ_k value and field, k has decreased to zero. For higher fields, the $k = 0$ condition forces θ_k to decrease once more. The minimum threshold is attained at $H_0 = H_c = 2200$ Oe with $\theta_k \approx 20°$ to 30°. These results are quite different from those which are normally assumed for transverse pumping in YIG and are directly attributable to the effect of the ΔH_k k-dependence on the threshold. This effect leads to (i) a rather wide field interval which extends well below the field for the minimum h_{crit} for which the unstable modes have $k = 0$, (ii) values of θ_k much larger than 45° at low field, and (iii) an increase in the field position of the butterfly curve minimum and a value of θ_k well below 45° at that point. It is also to be noted that the φ_k for the unstable modes is 0°, so that k is in the plane defined by the static field and the microwave polarization.

It may by noteworthy that the presently revealed large field region for $k = 0$ spin waves from $H_0 = 1700$ Oe upwards is precisely the same field region where a peculiar and unexplained series of dips in the butterfly curves has been observed by Jantz [3]. These data were obtained by a special technique in which the instability threshold was determined by sweeping the dc magnetic field with the microwave field amplitude held constant. The most important characteristic of the data was a peculiar fine structure in the microwave absorption [3, 7, 8], which was convincingly attributed to the spatial quantization of low-k spin-wave modes. The present theoretical results show that low-k modes do indeed yield the lowest threshold h_c over this entire field interval.

The lack of a good quantitative fit may be due to several factors. First, the spin-wave linewidth parameters for parallel pumping may not be quite right for transverse pumping. Second, it is to be recalled that second-order variational terms in the dynamic anisotropy field have been neglected. Such terms do contribute to the C_k^A and D_k^A factors in equation (35) of Part I (cf. [9]), and are likely to modify the theoretical curve in Fig. 4 to some extent.

4. Summary and Conclusion

A general formulation of spin-wave instability processes in magnetic insulators has been presented. The formulation includes the effects of cubic anisotropy on the threshold, as it is contained in the dispersion, the general spin-wave coupling terms, and

the uniform precession amplitude. The theory is valid for an arbitrary polarization of the microwave pumping field and ellipsoidal samples magnetized along a principal axis oriented in the crystallographic (110) plane. The other two principal axes of the ellipsoidal sample are taken to be perpendicular and parallel to the (110) plane, respectively.

It is shown that the effective anisotropy field is composed of static and dynamic elements, with components parallel to the saturation direction which are essential to the theory of instability processes. The previous approach in terms of an effective transverse anisotropy field, while adequate to explain FMR, is inadequate for instability theory. The free-energy formulation of the static and dynamic anisotropy field elements leads to general instability threshold equations for an arbitrary pump configuration. The theory reduces to previously derived expressions in the limits of zero anisotropy and parallel pumping. Specific numerical results agree well with the available experimental data.

Acknowledgements

The author is indebted to Dr. W. Jantz for stimulating and helpful discussions on the subject of this paper. Prof. W. Haubenreisser is gratefully acknowledged for helpful comments concerning the manuscript and the role of second-order variational terms in the effective field formulation.

References

[1] C. E. Patton and W. Jantz, IEEE Trans. Magnetics **14**, 698 (1978).
[2] J. C. Sethares, M. H. Seavey, T. G. Purnhagen, and M. R. Stiglitz, J. appl. Phys. **35**, 898 (1964).
[3] W. Jantz, Die Feinstruktur der Spinwelleninstabilitäten, Special Report, Inst. Angew. Festkörperphysik, Freiburg i. Br. 1974.
[4] Y. M. Yakovlev, Y. N. Burdin, Y. R. Shilnikov, and T. N. Bushueva, Soviet Phys. — Solid State **12**, 2475 (1971).
[5] M. Sparks, Ferromagnetic Relaxation Theory, McGraw Hill Publ. Co., New York 1964.
[6] C. E. Patton, J. appl. Phys. **40**, 2837 (1969).
[7] W. Jantz and J. Schneider, Solid State Commun. **9**, 69 (1971).
[8] W. Jantz and J. Schneider, phys. stat. sol. (a) **31**, 595 (1975).
[9] W. Haubenreisser, private communication.

(Received December 28, 1978)